The Science of Making Torque From Wind
Copenhagen, Denmark
June 18-20, 2014

High-fidelity Modeling of Local Effects of Damage for Derated Offshore Wind Turbines

Phillip W. Richards

Graduate Research Assistant, Daniel Guggenheim School of Aerospace Engineering. Georgia Institute of Technology, Atlanta, Georgia 30332-0150

E-mail: phillip@gatech.edu

D. Todd Griffith

Principal Member of the Technical Staff. Associate Fellow, AIAA. Sandia National Laboratories, Albuquerque, New Mexico 87123
Sandia National Laboratories is a multi-program laboratory managed and operated by Sandia Corporation, a wholly owned subsidiary of Lockheed Martin Corporation, for the U.S. Department of Energy's National Nuclear Security Administration under contract DE-AC04-94AL85000.

Dewey H. Hodges

Professor, Daniel Guggenheim School of Aerospace Engineering. Fellow, AIAA and AHS; member, ASME. Daniel Guggenheim School of Aerospace Engineering. Georgia Institute of Technology, Atlanta, Georgia 30332-0150

E-mail: dhodges@gatech.edu

Abstract. Offshore wind power production is an attractive clean energy option, but the difficulty of access can lead to expensive and rare opportunities for maintenance. As part of the Structural Health and Prognostics Management (SHPM) project at Sandia National Laboratories, smart loads management (controls) are investigated for their potential to increase the fatigue life of offshore wind turbine rotor blades. Derating refers to altering the rotor angular speed and blade pitch to limit power production and loads on the rotor blades. High-fidelity analysis techniques like 3D finite element modeling (FEM) should be used alongside beam models of wind turbine blades to characterize these control strategies in terms of their effect to mitigate fatigue damage and extend life of turbine blades. This study will consider a commonly encountered damage type for wind turbine blades, the trailing edge disbond, and show how FEM can be used to quantify the effect of operations and control strategies designed to extend the fatigue life of damaged blades. The Virtual Crack Closure Technique (VCCT) will be used to post-process the displacement and stress results to provide estimates of damage severity/criticality and provide a means to estimate the fatigue life under a given operations and control strategy.

1. Introduction

Offshore wind power production is an attractive clean energy option, but the difficulty of access can lead to expensive and rare opportunities for maintenance. The Structural Health and

Prognostics Management (SHPM) project at Sandia National Laboratories (see [1], [2]) has developed a roadmap to address these issues, in particular technology development to reduce operations and maintenance (O&M) costs and increase energy capture. In one element of this roadmap, smart loads management (controls) are investigated as simple fatigue considerations (under this project as well as in other works) and the potential has been identified to derate a damaged turbine via smart loads management to significantly increase its fatigue life. Derating refers to altering the rotor angular speed and blade pitch to limit power production and loads on the rotor blades. These studies typically have utilized simplified beam models to evaluate new operations and controls strategies and point to a reduction in tower or blade section loading to show the success of the strategy.

High-fidelity analysis techniques such as finite element modeling should be used alongside these beam models to quantitatively and accurately characterize each strategy in terms of its effect to mitigate fatigue damage and extend life of turbine blades. High-fidelity analysis is critical in the case of damaged blades due to local effects in the damaged area of the blade. This study will consider a commonly encountered damage type for wind turbine blades, the trailing edge disbond, and show how finite element modeling can be used to quantify the effect of operations and control strategies designed to extend the fatigue life of damaged blades. The finite element modeling strategy will use a multiscale procedure, with a "global" shell model analysis for behavior of most of the blade, and a "local" model to analyze the behavior in the vicinity of the damage. Both models will represent the damage using nonlinear contact elements that accurately capture opening and closing behavior of the disbonds. The Virtual Crack Closure Technique (VCCT) [3] will then be used to post-process the displacement and stress results from the finite element analyses to provide estimates of damage severity and damage growth rates. The results of this process will indicate the criticality of common damage features with respect to damage location and type of loading, as well as provide a means to estimate the fatigue life or growth of damage under a given operations and control strategy.

2. Background

A general cost-benefit analysis of offshore wind energy is presented by Snyder and Kaiser [4]. This analysis identifies the relative cost and risk of offshore turbines (compared with onshore) as a main barrier for acceptance of offshore wind, and highlights the larger percentage of operational and maintenance costs of the total offshore cost of energy (compared with onshore). A major goal of the SHPM project is to present operational and control strategies for offshore wind farms that will minimize the total cost of energy, by avoiding blade damage or mitigating blade damage growth with smart loads management.

The purpose of the smart loads management system is to (a) avoid a catastrophic failure through advance warning, (b) plan cheaper maintenance and (c) increase energy capture by avoiding shutdown. The resulting strategies will consist of decisions to shut down, operate the turbine normally, or operate potentially damaged turbines in a safe way. The recommendation to operate damaged turbines must justify the risk of further damage to the turbine based on the local sensitivity analysis results and the potential to increase the annual energy production (AEP). where inspection and maintenance can be difficult. An effective prognostic control strategy will therefore reduce the total cost of energy by reducing O&M costs as well as increasing power production for offshore wind farms.

2.1. Operation and Maintenance Strategies

Decisions of how to operate a turbine should be made in conjunction with an inspection and maintenance scheduling strategy. An overview of maintenance management is given by [5]. Rangel-Ramirez and Sorensen [6] applied a risk-based inspection strategy from offshore oil industry to offshore wind farms, showing that operational decisions regarding inspections should

consider turbulent wake effects of the farm as a whole. Zhang et al. [7] use a wake-loss model and historical data to define an inspection model that accounts for the wake of each turbine. This inspection model would use weather reports when available and historical data when necessary to make up-to-date decisions. This way wind turbines heavily affected by the wake(s) of one or more other turbines or whose wake affects other turbines would be shut down in favor of turbines operating optimally. This model in particular would be an ideal starting point for an operational strategy that includes damage tolerance considerations. A damaged turbine that is forecasted to be partially within the wake of another, for example, would likely remain shut down, while a damaged turbine that is forecasted to be within a clear inflow would then operate under a prognostic control system. Wenjin et al. [8] proposed a predictive maintenance strategy based on modeling the blade deterioration with Monte Carlo simulations. This is again similar to the proposed operations strategy, except that the damage detection efforts of the SHPM project are intended to augment or replace blade deterioration models [9, 10].

2.2. Control System Considerations

Under "normal" operation, a wind farm is operated to maximize power production. Modern wind turbines of 5 MW or larger are typically controlled in yaw, pitch, and rotor angular speed to optimize their power production capability. The yaw control is used to align the rotor with the wind direction, while pitch and speed controls are primarily used to control aerodynamic loads and generator performance. The rotational speed of the turbine is controlled via torque control of the generator. The pitch and speed controls of each turbine can either be used individually to maximize the power output of each individual turbine, or in a collective sense to maximize the power output of the wind farm as a whole [11, 12, 13]. For this research, the NREL 5 MW baseline design [14] will be considered as a representative offshore turbine design with yaw, pitch, and rotor speed controls.

Under "damaged" operation, the control strategies will be used to produce power production while alleviating loads on damaged blades. Bossanyi has studied the blade load reduction problem extensively [15, 16, 17, 18]. One example of individual blade control design using sliding-mode control is given by Xiao et al. [19]. Pitch control is often used to mitigate vibrations of offshore platforms, including the use of individual blade pitch control as in [20, 21, 22, 23, 24], and structural control methods as in [25]. These vibrations create fatigue damage of the foundation [26], so are often the focus of offshore wind turbine control design efforts. Accurate platform fatigue analysis requires nonlinear modeling of the wave conditions [27]. In general, the structural health monitoring systems should be integrated with the operation and controls of the wind turbine as demonstrated by Frost et al. [28]. A good prognostic control strategy would address all of these issues in addition to possible blade damage, but these considerations are beyond the scope of the current research. It is enough to say that pitch control techniques have been shown to have a wide variety of applications to blade-load reduction.

The simplest example of a load-reducing, pitch-control method is to utilize the available pitch-control system to control blade RPM and pitch to limit the power production to a lower level [9, 28]. For this research, the derating was accomplished by holding the RPM constant above the windspeed when the power production exceeds its derated level at a 0° pitch setting, and then using the pitch controller to maintain the power production as the windspeed increases. For the NREL 5 MW baseline turbine, a 50% derating strategy, and a Rayleigh wind profile with average windspeed of 10 m/s, the annual energy production (AEP) is reduced from $\approx 2.5 \times 10^7$ kWh to $\approx 1.5 \times 10^7$ kWh. The power production and control scheduling required to achieve this derating is shown in Fig. 1 as well as the root bending moment. The reduction in AEP is less than the reduction in maximum power level because at low windspeed the power production is not changed; the power production is only limited in this case at 9 m/s and above. The loads in terms of maximum bending moments at the root of the blade were reduced by approximately

50%. The advantage to using a simple "derating" method is that it would only involve a change in the software of currently operating offshore turbine control systems, and therefore could be easily retrofitted into pre-existing designs.

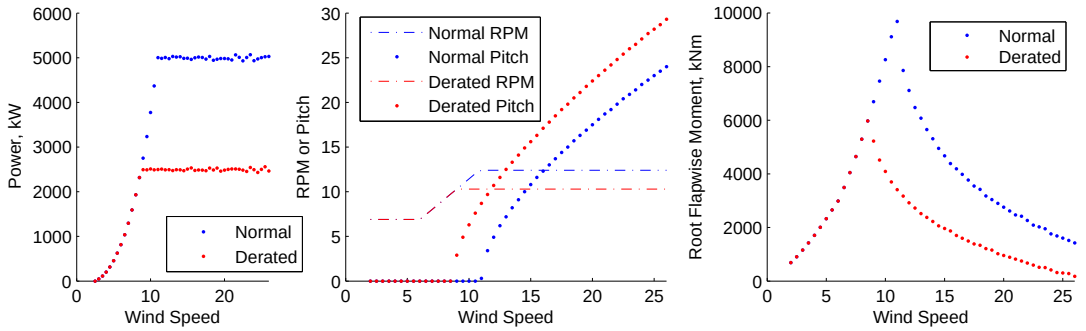

Figure 1: Derated (50% power level) power productioncontrol scheduling, and root bending moment compared with normal/baseline operation.

2.3. Damage Tolerance Analysis within a Prognostic Control Framework

The study of damage tolerance is a field in and of itself, with the damage tolerance of composites being a currently quite active. A good review of the subject is given by Fan et al. [29]. Damage tolerance predictions may be divided into two categories: stress-based approaches and energy-based approaches. Stress-based approaches are quite useful for isotropic, ductile materials; but the anisotropic, brittle nature of composites leads to singular stress fields and damage mechanisms that are very different from those in metallic materials. Therefore, energy-based methods are often preferred for prediction of damage initiation and growth in composites. These energy-based methods involve calculation of the Strain Energy Release Rate (SERR), which is an estimate of the strain energy released when a crack opens from length a to $a + da$ and is commonly referred to by the symbol G. Regardless of the material, the field of damage tolerance typically recognizes three distinct modes of crack propagation, referred to as Mode I, II, and III. Therefore, the energy-based prediction method will typically provide three values of G for each mode, denoted G_I, G_{II}, and G_{III}. Fracture is assumed to occur with energy-based methods when some combination of the G values for each mode reaches a material-dependent parameter known as the critical energy release rate G_c. The way in which the G values are combined depends on mode-mixity models, which are typically extracted from experimental data.

One popular energy-based method is the Virtual Crack Closure Technique (VCCT), which is reviewed by Krueger [3]. The VCCT essentially operates on the assumption that as the crack opens from size a to $a+da$, the internal forces at the crack tip do not change significantly. When attempting to close a crack from length $a+da$ to length a, the energy required will be the opened displacements multiplied by the internal forces that resist the closure. The main assumption of the VCCT allows the forces at the crack tip to be used in this calculation. Therefore, the resulting formulas for the SERR in modes I, II, and III are, respectively,

$$G_I = \frac{1}{2\Delta a} F_y(u_y - \bar{u}_y) \qquad G_{II} = \frac{1}{2\Delta a} F_z(u_z - \bar{u}_z) \qquad G_{III} = \frac{1}{2\Delta a} F_x(u_x - \bar{u}_x) \tag{1}$$

where u_i are the displacements of the upper surface and $\bar{u}_i$ are the displacements of the lower surface. Here, y refers to the direction perpendicular to the line of the crack in the "opening" direction, z refers to the direction along the line of the crack, and x refers to the direction perpendicular to the opening direction and the line of the crack. This method has been recently applied to the problem of trailing edge disbonds by Eder et al. [30] to predict damage onset

location and assess the effect of loading directions on the blade. They concluded that Mode III is the governing Mode of fracture for this type of damage and that flapwise shear and torsion are the most important load cases.

The VCCT method is valid for linear problems, and does not account for some typical damage phenomena such as fiber bridging. For this study, it is assumed that the damage lies within the adhesive and therefore the linear nature of the VCCT is acceptable. Because the crack is assumed to lie within the adhesive, any issue with the VCCT due to a bimaterial interface was avoided.

3. Approach and Results

This research will take a multiscale analysis approach to the problem. The Sandia National Laboratories Numerical Modeling and Design (NuMAD) tool is an open-source tool for analyzing realistic composite wind turbine blades [31]. This tool has the capability of transforming a traditional beam and section definition of a wind turbine model into a high-fidelity ANSYS shell model. Since this capability is readily available to interested academic and industry parties and it produces a high-fidelity model of the blade as a whole, this shell modeling capability was utilized for this study as the "global" analysis. The shell model does not have a sufficiently refined mesh near the trailing edge, which is the area of interest of this research, so the global analysis needs to be supplemented with a "local" analysis as well. After the VCCT is verified with a simple example and the mesh dependency of the technique is established, the criticality of trailing edge disbonds with respect to damage location and size is examined for both the normal operational strategy and the derated strategy. The comparisons will be made at the rated windspeed, where there is a significant difference in loading between the two operational strategies. To demonstrate the method, only the "global" analyses are shown here, so that the qualitative nature of the trends can be established.

3.1. Validation for Isotropic Section

To validate the VCCT method, a classic example was set up with isotropic materials. The example consists of a horizontal crack in a thin, square plate, with a vertical displacement condition applied to the upper and lower boundaries. The example has a known analytical solution for the SERR, which can be compared to the VCCT results to validate the method. The analytical solution is:

$$G_I = \frac{\pi \sigma^2 a}{E} \tag{2}$$

Figure 2 compares the grid convergence of this simple example. The general trend of the behavior is captured with the smallest mesh density, which lends credence to the following trends recovered using only the "global" shell model. For this study the shell model was used to examine the qualitative behavior of the SERRs, and further work will refine the analyses quantitatively.

3.2. Global NuMAD Shell Model

The damage location on the wind turbine blade, the coordinate system and the possible directions of damage propagation are depicted in Fig. 3. The NuMAD tool was used to generate an ANSYS model from a description of the NREL 5MW blade geometry and materials. The ANSYS shell model was modified by removing the connectivity of elements adjacent to the trailing edge, adding coincident nodes along the trailing edge, and reconnecting the upper elements to the new coincident nodes. Then, COMBIN elements, which are essentially nonlinear springs, were used to connect the coincident nodes. The stiffness behavior of the COMBIN elements was modified to have zero stiffnesses in the "X" (chordwise) and "Z" (spanwise) directions and in the positive "Y" (flapwise) directions, but a very high stiffness in the negative

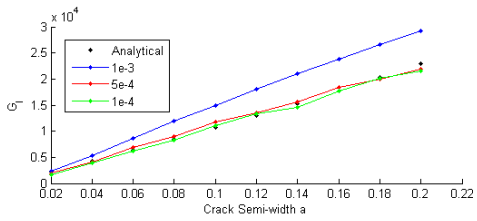

Figure 2: VCCT results for rectangular sample with horizontal mid-plane crack.

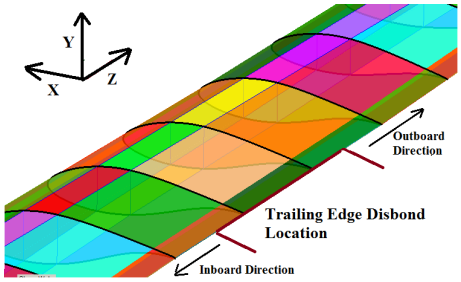

Figure 3: Depiction of trailing edge disbond location on blade, and possible directions of damage propagation.

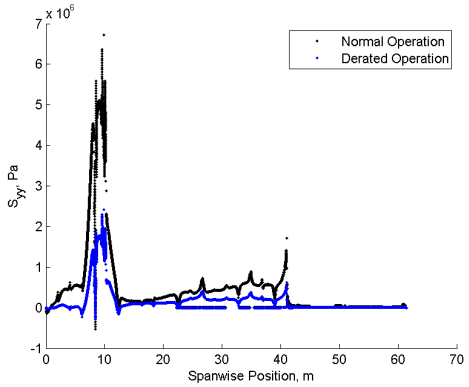

Figure 4: Stress results for σ_{yy} along the bond line for the baseline model during normal operation and derated to 50% power level.

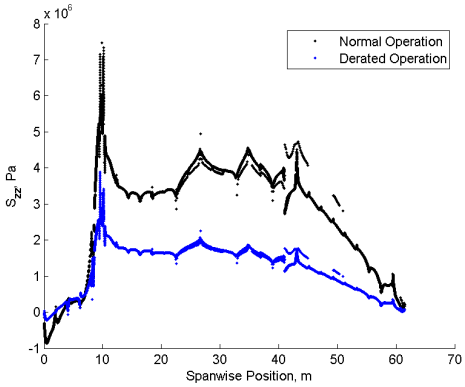

Figure 5: Stress results for σ_{zz} along the bond line for the baseline model during normal operation and derated to 50% power level.

"Y" direction. This approach was verified to model the opening/closing behavior of the disbonds. The loading at rated windspeed during normal or derated operation was calculated using WT_Perf, which is a blade-element/momentum theory solver for wind turbines provided by the National Renewable Energy Laboratory (NREL). The distributed loading from the WT_Perf model was then applied to the ANSYS model via the application of point loads at each external node in the ANSYS model. The value of the point loads was obtained by performing a least-squares regression to determine a value of forces at each node to produce the desired distributed forces and twisting moments. The capability to map distributed loads to the ANSYS model is included in the NuMAD functionality [32].

3.2.1. Healthy Blade Stress Results The healthy baseline stress values σ_{yy}, σ_{zz}, σ_{yz}, and σ_{xz} are shown along the bond line in Figs. 4 – 7, respectively. The stress components σ_{yy} and σ_{yz} are related to opening of the crack due to Mode I, and σ_{zz} and σ_{zx} are related to opening of the crack in modes II and III. Note that these healthy stress components show major perturbations in the vicinity of $R = 10$ m and $R = 40$ m locations. These locations happen to coincide with the locations where the ANSYS model blends from circular cross sections to blunt trailing edges ($\approx$10 m span) and from blunt trailing edges to sharp trailing edges ($\approx$ 40 m span). These transition points are shown in Fig. 8. These regions of high stress in the undamaged blade are therefore of interest when it comes to analysis of damage criticality.

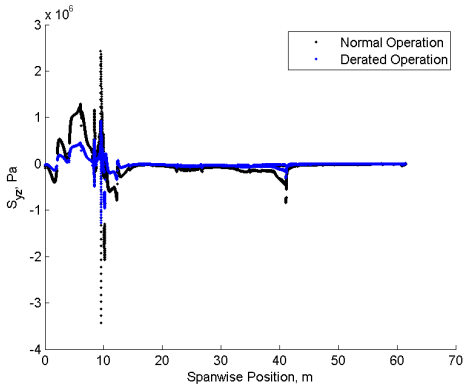

Figure 6: Stress results for σ_{yz} along the bond line for the baseline model during normal operation and derated to 50% power level.

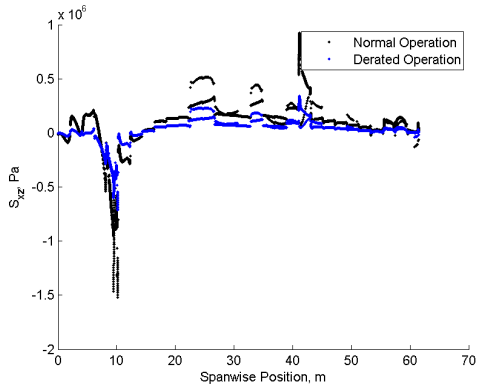

Figure 7: Stress results for σ_{xz} along the bond line for the baseline model during normal operation and derated to 50% power level.

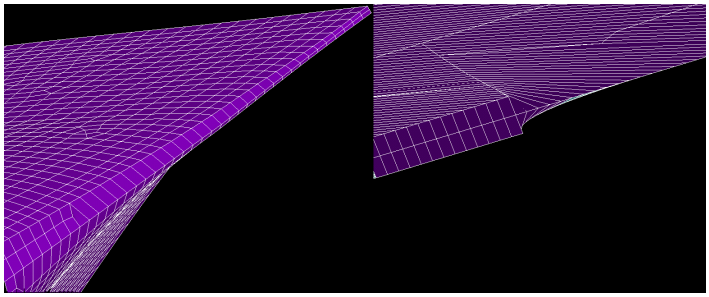

Figure 8: Geometry transitions from circular cross sections to airfoil sections with blunt trailing edges (left) and transition from blunt trailing edges to sharp trailing edges (right).

3.2.2. SERR Calculations Under Normal Operation The SERR was calculated from the "global" ANSYS shell model by using the resulting nodal forces at the crack tip and the opened displacements of the nodes just within the crack tip. At this time, the "global" results are not fully trusted to be numerically accurate to the actual SERRs within the propagation, but it is assumed that these results are sufficient for demonstrating general trends. The results for SERRs of the healthy model are then shown in Figs. 9 – 14. Note that the results labeled "inboard" would represent the SERR for propagating the crack towards the hub, while results labeled "outboard" represent SERRs for crack propagation towards the tip of the blade. These show that the G_I values for the inner and outer crack tip are very high when the crack begins around the 10 m span location, and then drop suddenly as the start of the crack moves from 11 m to 12 m. After this the G_I values increase with the starting position of the crack. The G_{II} and G_{III} values generally increase both with increasing a and also with increasing starting position.

3.2.3. SERR Calculations under Derated Operation The loading at the rated windspeed during derated operation was calculated using WT_Perf and again mapped to the ANSYS model via nodal point loads. The derating involved setting the maximum power level to 2.5 MW and allowing the turbine controls to behave as if this were the rating of the wind turbine. The result was a slight adjustment to the RPM and pitch scheduling of the wind turbine (vs. windspeed). Figures 15 and 16 show selected SERR results for the turbine under this type of derating, at the rated wind speed, where the root bending moment has been reduced by a factor of 2.8.

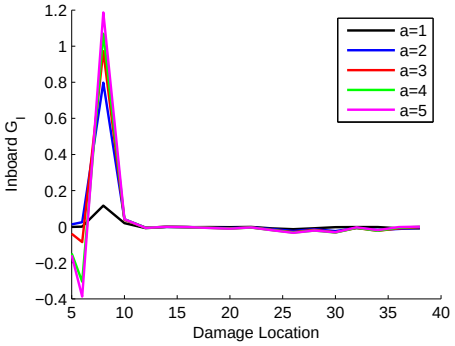

Figure 9: SERR (J/m^2) for Mode I fracture of the inner crack tip for various starting positions (11 – 20 m) and crack lengths (0.5 – 5 m), normal operation, rated windspeed.

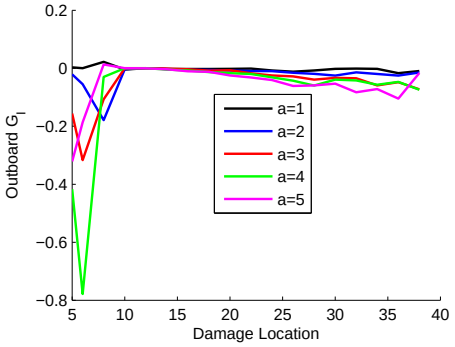

Figure 10: SERR (J/m^2) for Mode I fracture of outer crack tip for various starting positions (11 – 20 m) and crack lengths (0.5 – 5 m), normal operation, rated windspeed.

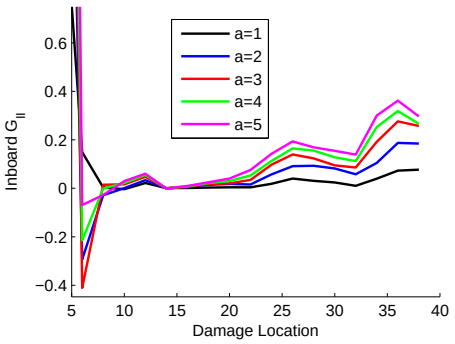

Figure 11: SERR (J/m^2) for Mode II fracture of the inner crack tip for various starting positions (11 – 20 m) and crack lengths (0.5 – 5 m), normal operation, rated windspeed.

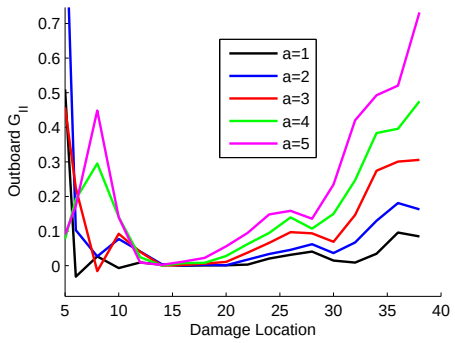

Figure 12: SERR (J/m^2) for Mode II fracture of the outer crack tip for various starting positions (11 – 20 m) and crack lengths (0.5 – 5 m), normal operation, rated windspeed.

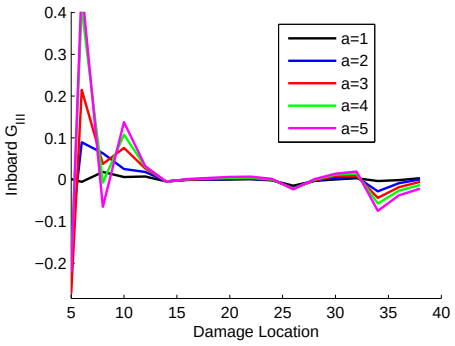

Figure 13: SERR (J/m^2) for Mode III fracture of the inner crack tip for various starting positions (11 – 20 m) and crack lengths (0.5 – 5 m), normal operation, rated windspeed.

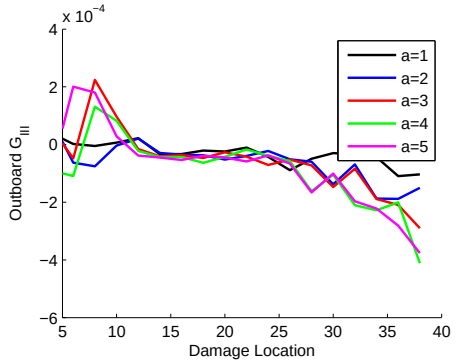

Figure 14: SERR (J/m^2) for Mode III fracture of the outer crack tip for various starting positions (11 – 20 m) and crack lengths (0.5 – 5 m), normal operation, rated windspeed.

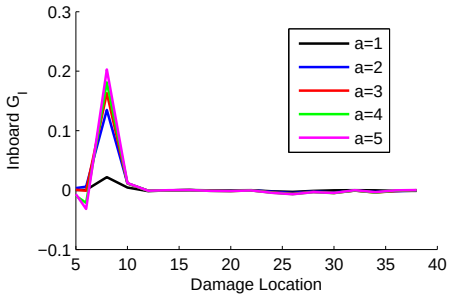

Figure 15: SERR (J/m^2) for Mode I fracture of the inner crack tip for various starting positions (11 – 20 m) and crack lengths (0.5 – 5 m), derated operation, rated windspeed.

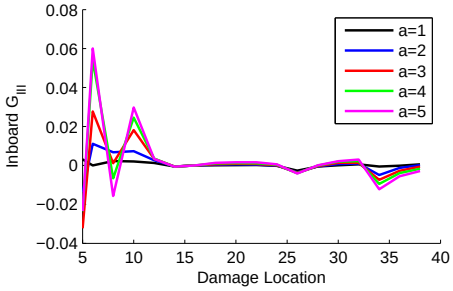

Figure 16: SERR (J/m^2) for Mode III fracture of the inner crack tip for various starting positions (11 – 20 m) and crack lengths (0.5 – 5 m), derated operation, rated windspeed.

These figures demonstrate that the derated values followed trends similar to those under normal operation but with reduced magnitude. This was true for each of the outputs shown in the previous section. For G_I, the calculated SERRs were reduced by around a factor of 7 by the derating process, and the SERR values for G_{II} and G_{III} were reduced by factors of around 5 by the derating process for this wind speed.

4. Conclusions

A framework has been established for high-fidelity analysis of damage severity and demonstrated for the common damage type of trailing-edge disbonding. These efforts demonstrated that the most critical area in terms of damage onset is in the vicinity of the 10 m span location, which happens to be where the cross-sectional shape transitions from circular to airfoil-shaped. Therefore, this transition point is a key area of interest in damage tolerance analysis or designs that account for damage tolerance. Of course, the sharp corner in Fig. 8 may be due to mesh coarseness, but in general if this transition area can be smoothed out or reinforced, it may produce a more damage tolerant blade. In this research, the area of stress concentration in the baseline (healthy) bond line also had the highest SERR values. This implies that designing the blade considering the healthy stress results only may also be a strategy for producing damage tolerant designs.

This research also demonstrated the application of a derating controls strategy to reduce the SERRs of this common damage type. Although values of G_I were reduced significantly, a smaller reduction was found in G_{II} and G_{III}. Eder et al. [30] identified Mode III as the dominant failure mode for damage of this type. A more advanced derating strategy that also targets G_{II} and G_{III} will likely be more effective.

This high-fidelity analysis framework will be used to evaluate new control strategies or potentially damage tolerant designs. In order to provide accurate predictions of damage onset and growth using this model, it must first be supplemented by a local analysis procedure in order to enhance the accuracy of the results. The SERR results will be used as inputs to a damage onset or growth model. The analysis will be conducted for each operating wind speed, and a probability law will be used to combine the growth rates into a meaningful result; also, dynamic analysis of extreme events will be performed.

Then, the framework will be suitable to provide operations and maintenance guidelines for wind turbines under different types of operational strategies. These guidelines will help operators avoid catastrophic failure of turbine blades through advance warning, plan efficient maintenance operations and increase energy capture by avoiding shutdown. The smart loads management

system, if possible, will utilize control architectures of modern offshore wind turbines and will therefore be useful for operators of existing state-of-the-art wind plants.

References

[1] Griffith D T, Yoder N, Resor B, White J and Paquette J 2012 Structural health and prognostics management for offshore wind turbines: An initial roadmap Tech. Rep. SAND2012-10109 Sandia National Laboratories
[2] Griffith D T, Yoder N C, Resor B, White J and Paquette J 2013 *Wind Energy*
[3] Krueger R 2004 *Applied Mechanics Review* **57**
[4] Snyder B and Kaiser M J 2009 *Renewable Energy* **34** 1567–1578
[5] Frangopol D M, Saydam D and Kim S 2012 *Structure and Infrastructure Engineering* **8** 1–25
[6] Rangel-Ramirez J G and Sorensen J D 2012 *Structure and Infrastructure Engineering* **8** 473–481
[7] Zhang J, Chowdhury S, Zhang J, Tong W and Messac A 2012 *12th AIAA Aviation Technology, Integration, and Operations (ATIO) Conference and 14th AIAA/ISSM. Indianapolis, Indiana*
[8] Wenjin Z, Fouladirad M, Berenguer C *et al.* 2013 *Annual Reliability and Maintainability Symposium-RAMS 2013*
[9] Myrent N, Kusnick J, Barrett N, Adams D and Griffith D 2013 Structural health and prognostics management for offshore wind turbines: Case studies of rotor fault and blade damage with initial om cost modeling Tech. Rep. SAND2013-2735 Sandia National Laboratories
[10] Myrent N J, Adams D E and Griffith D T 2014 *32nd ASME Wind Energy Symposium. National Harbor, Maryland*
[11] Marden J R, Ruben S D and Pao L Y 2012 *Proceedings of the 50th AIAA Aerospace Sciences Meeting, Nashville, TN.*
[12] Gonzalez J S, Payan M B and Santos J R 2013 *Eurocon, 2013 IEEE* (IEEE) pp 1129–1134
[13] Kusiak A and Song Z 2010 *Renewable Energy* **35** 685–694
[14] Jonkman J, Butterfield S, Musial W and Scott G 2009 Definition of a 5-mw reference wind turbine for offshore system development. Tech. Rep. NREL/TP-500-38060
[15] Bossanyi E 2000 *Wind Energy* **3** 149–163
[16] Bossanyi E 2003 *Wind Energy* **6** 119–128
[17] Bossanyi E 2003 *Wind Energy* **6** 229–244
[18] Bossanyi E 2005 *Wind Energy* **8** 481–485
[19] Xiao S, Yang G and Geng H 2013 *ECCE Asia Downunder (ECCE Asia), 2013 IEEE* (IEEE) pp 227–232
[20] Wang L, Wang B, Song Y and Zeng Q 2013 *Advances in Vibration Engineering* **12** 377–390
[21] Larsen T J and Hanson T D 2007 *Journal of Physics: Conference Series* **75**
[22] Jonkman J M 2008 *2008 ASME Wind Energy Symposium, Reno, Nevada.*
[23] Christiansen S, Bak T and Knudsen T 2013 *IEEE Transactions on Control Systems Technology* **6** 4097–4016
[24] Namik H and Stol K 2010 *Wind Energy* **13** 74–85
[25] Rotea M, Lackner M and Saheba R 2010 *48th AIAA Aerospace Sciences Meeting and Exhibit, Orlando, Florida*
[26] Yamashita A and Sekita K 2004 *Proceeding of the 14th International Offshore and Polar Engineering Conference* pp 166–171
[27] Trumars J M, Tarp-Johansen N J and Krogh T 2005 *24th International Conference on Offshore Mechanics and Arctic Engineering* (ASME)
[28] Frost S A, Goebel K, Balas M J and Henderson M T 2013 *51st AIAA Aerospace Sciences Meeting Including the New Horizons Forum and Aerospace Exposition. Grapevine, TX, USA*
[29] Fan X, Sun Q and Kikuchi M 2010 *Journal of Solid Mechanics Vol* **2** 275–289
[30] Eder M, Bitsche R, Nielsen M and Branner K 2013 *Wind Energy* **17**
[31] Berg J C and Resor B R 2012 Numerical manufacturing and design tool (numad v2.0) for wind turbine blades: Users guide Tech. Rep. SAND2012-7028 Sandia National Laboratories
[32] Berg J, Paquette J and Resor B 2011 *52nd AIAA/ASME/ASCE/AHS/ASC Structures, Structural Dynamics, and Materials Conference. Denver, Colorado*